# Two-Color Resonant Four-Wave Mixing Spectra of the $C^2\Sigma^+-X^2\Pi(1-1)$ Band of CH in a Flame

**Xinghua Li, Awadhesh Kumar, Chih-Chang Hsiao, and Yuan-Pern Lee***

*Department of Chemistry, National Tsing Hua University, 101, Sec. 2, Kuang Fu Road, Hsinchu, Taiwan 30043*

*Received: March 25, 1999; In Final Form: May 21, 1999*

We investigated predissociative transitions $C^2\Sigma^+$ ($v' = 1$)−$X^2\Pi$ ($v'' = 1$) of CH in an oxyacetylene flame with the two-color resonant four-wave mixing technique in which two grating beams are in resonance with the C−X transition and the probe beam is resonant with a selected A−X transition. Six branches of the C−X system are spectrally resolved for the first time; in total 124 lines detected in this work correspond to excitation of the C state up to $N' = 23$. Observed wavenumbers are fitted to yield improved spectral parameters of the $C^2\Sigma^+$ ($v = 1$) state; one additional centrifugal distortion parameter $L_V$ is evaluated significantly. These data are combined with lines of C−X (0−0) and (2−2) bands to provide improved characterization of the C state of CH. For all lines of the C−X (1−1) band, the line widths are nearly identical. Predissociation mechanisms of the C state are discussed.

## I. Introduction

The carbon hydride (CH) radical is an important constituent of various environments such as the sun,[1] interstellar space,[2,3] and flames.[4] Numerous spectral investigations of the systems $A^2\Delta-X^2\Pi$ and $B^2\Sigma^--X^2\Pi$ are reviewed.[5−10] The $X^2\Pi$, $A^2\Delta$, and $B^2\Sigma^-$ states are well characterized.

The $C^2\Sigma^+-X^2\Pi$ system near 310 nm was observed more than 70 years ago.[11,12] The C state of CH plays an important role in many respects. Moore and Broida[13] identified the C−X system in the solar spectrum. Astrophysical implications of the predissociation of the C state, which results in rapid destruction of CH under interstellar radiation, is discussed.[14] Visualization of CH molecules in a turbulent flame is realized by means of laser-induced fluorescence of the C−X system.[15,16]

The vibronic state of $C^2\Sigma^+$ is poorly characterized except for $v = 0$. Heimer,[17] employing a graphite arc source in a hydrogen atmosphere, reported 159 lines of the C−X (0−0) band with excitation up to $N' = 27$ of $C^2\Sigma^+$ ($v = 0$), but the C−X (1−1) band was not resolved. Gerö[18] reported measurements of the systems C−X (0−0), (1−1), and (2−2) of CD. Herzberg and Johns[19] observed the C−X (2−2) band of CH and extended measurements of the CD bands to (4−4). Using a frequency-doubled cw ring dye laser with a bandwidth of ∼0.5 MHz to excite CH in a molecular beam, Ubachs et al.[20] resolved hyperfine structure in the C state and determined accurate rotational, spin-rotation, and hyperfine parameters of the $C^2\Sigma^+$ ($v = 0$) state. Recently, Bembenek et al.[21] analyzed the C−X (0−0) system of $^{13}$CH produced in a Geissler tube.

Predissociation of the C state was observed.[14,17,19−24] The slower component ($\tau \approx 150$ ns) of a biexponential decay of the C−X emission reported previously[14] is shown to result from air impurities.[23] Based on measurements of widths of emission lines with a narrow-band laser, Ubachs et al.[20] reported that $F_1$ states of $v = 0$ have a constant lifetime $3.7 \pm 1.0$ ns, whereas for $F_2$ states, the lifetime increases slightly with $N$ and reaches $8.0 \pm 1.5$ ns at $N = 11$.

The $C^2\Sigma^+$ ($v = 1$) state is poorly characterized, presumably because of spectral interference and its predissociative nature. A spectral technique that is both free from interference and extremely sensitive to allow detection of short-lived predissociative states is thus desirable. We detected highly predissociative levels of the $B^2\Sigma^-$ state of CH ($\tau$ as small as 1 ps) in a flame with the two-color resonant four-wave mixing (TC-RFWM) technique.[25,26] The number of observed lines of transitions B−X (0−0) and (1−0) is nearly twice as many as in previous reports, consequently resulting in improved spectral parameters of the B state.

TC-RFWM involves interaction of three input laser beams at a small angle with a medium to generate a highly collimated, coherent laser signal through induced nonlinear polarization associated with the third-order susceptibility $\chi^{(3)}$. The TC-RFWM technique may be understood as a picture of a transient grating.[27] Two temporally coincident laser beams (called grating beams) with an identical wavelength in resonance with a molecular transition create transient modulation of population or phase in a medium. This grating-like modulation diffracts a third (probe) laser beam in resonance with another molecular transition that shares a common level with that of the grating beams. Formation of the transient grating is typically independent of mechanisms of loss from excited levels; hence, TC-RFWM has an advantage in detecting nonfluorescent or unstable states. The double resonance nature provides distinct selectivity, thus eliminates interference from other transitions or species. These characteristics, combined with the fact that the TC-RFWM signal is coherent and polarization selective, make TC-RFWM a versatile tool to detect predissociative or congested transitions.

We report here new measurements of the C−X (1−1) band using TC-RFWM; the analysis yields improved spectral parameters of the state $C^2\Sigma^+$.

* To whom correspondence should be addressed. E-mail: yplee@net.nthu.edu.tw. Fax: 886-3-5722892.

† Jointly appointed by the Institute of Atomic and Molecular Sciences, Academia Sinica, Taipei, Taiwan.

10.1021/jp991027b CCC: $18.00 
Published on Web 07/16/1999

## II. Experiments

To apply the TC-RFWM technique to detect the C−X (1−1) transition, we employed a V-type double resonance scheme with a ground-state grating. As the $C^2\Sigma^+$ state is predissociative, the C−X transition is chosen as the grating-forming transition, whereas a band A−X is used as the probe transition. The brief lifetime of the C state does not affect formation of a transient grating resulting from population modulation of the X state; the signal originates from levels of the A state that are nonpredissociative. The intense A−X transition allows use of a probe beam of small intensity; hence, scattered light due to the probe beam is diminished. We select typically a probe wavelength in resonance with a known A−X transition to mark a specific level of the X state and scan the wavelength of the grating laser; an enhanced signal appears when the grating and the probe transitions share a common lower level in the X state.

The experiment is similar to what has been described before.[25,26] In brief, the output of a Nd:YAG pumped dye laser (Spectra-Physics, GCR-5 with injection seeder and PDL-3 with DCM special dye) with a typical line width about 0.08 $cm^{-1}$ is frequency doubled with a Quanta-Ray WEX-1 wavelength extender. The frequency-doubled output is split into two beams ($\omega_1$ and $\omega_2$) of comparable intensity to provide grating beams. The output of an excimer-pumped dye laser (Lambda-Physik LPX105i and FL3002 with Stilbene 3 dye) with a typical line width of about 0.2 $cm^{-1}$ is turned a to known CH $A^2\Delta-X^2\Pi$ transition,[9,10] as a probe beam ($\omega_3$). The timing among these two lasers and the data acquisition system are controlled with a pulse-delay generator (Stanford Research Systems, DG535). The grating and probe beams are arranged in a phase-matched forward-box geometry and cross in the CH-rich zone of an oxyacetylene flame. A *YXXY* cross-polarization scheme is typically used because it greatly minimizes the interference from scattered light; the polarization directions (*X* and *Y*) are listed in order of beams 4, 1, 3, and 2, with beam 4 indicating the signal beam and beams 1 and 2 the grating beams. Typical energies less than 20 $\mu$J for each of the three beams are used in order to minimize the effect of saturation broadening. The wavelengths of laser beams are calibrated with an Fe−Ne optogalvanic cell (Hamamatsu L2783-26-NE-FE) in combination with a wavemeter (Burleigh WA-5500, accuracy 0.2 $cm^{-1}$). The signal beam ($\omega_4$) is spatially filtered using a set of pinholes and lenses and spectrally filtered with an interference filter before detection with a photomultiplier mounted. The signal is averaged with a gated boxcar integrator (Stanford Research Systems, SR250) and data are sent to a PC for further processing.

Our source of CH is an oxyacetylene flame produced with a standard welding torch. To probe the CH-rich region of the flame, we mounted the torch on a *xyz* translator to optimize the signal.

## III. Results and Discussion

If we neglect hyperfine splitting due to spin of the hydrogen nucleus, there are six main branches of the transition $C^2\Sigma^+-X^2\Pi$. Figure 1 depicts partial energy levels of $C^2\Sigma^+$, $A^2\Delta$, and $X^2\Pi$ states and corresponding transitions. In this experiment, a ground-state grating scheme with $X^2\Pi$ serving as a common state for double resonance is employed. For example, with the probe laser set at a rovibronic line $Q_{1f}(N'')$ of the A−X system, a line $Q_1(N'')$ of the C−X system is detected on scanning the wavelength of the grating beams. Similarly, with the probe laser in resonance with a line either $P_{1e}(N'')$ or $R_{1e}(N'')$ of A−X, a pair of lines $P_1(N'')$ and $R_1(N'')$ of C−X are observed. We use

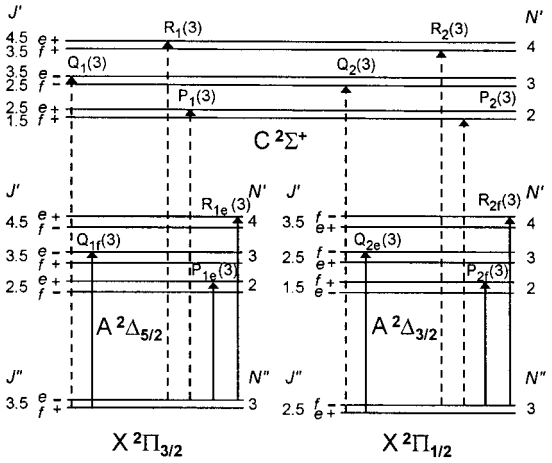


**Figure 1.** A partial energy level diagram of CH showing allowed C−X transitions for each probed A−X transition in the TC-RFWM experiments. Dashed arrows are grating transitions and solid arrows are probe transitions.

the standard notation $\Delta J(N'')$ for the transition and denote transitions associated with spin−orbit states $X^2\Pi_{3/2}$ and $X^2\Pi_{1/2}$ with subscripts "1" and "2". The parities "e" and "f" of $\Lambda$ doublets are labeled according to ref 28.

The C−X (0−0) band is well characterized; hence, we concentrate our work on the C−X (1−1) band. Wavenumbers of lines in the C−X (0−0) band measured in this work are nearly identical to those reported by Heimer.[17] Heimer also reported 50 lines of C−X (1−1) unresolved for spin−orbit components. We recorded 124 lines for this system with $N'$ excited up to 23, as listed in Table 1. Representative spectra appear in Figure 2. In our previous experiment on the B−X system using TC-RFWM, we observed twice as many lines as reported previously and extended observed predissociative levels of $B^2\Sigma^-$ from $N' = 15$ to 21 and $N' = 7$ to 12 for $v' = 0$ and $v' = 1$ states, respectively. However, although we resolve spin−orbit splitting in the C−X (1−1) band with improved detectivity, the number of levels of the C state observed in this experiment is similar to that reported by Heimer.[17] Predissociation of the $C^2\Sigma^+$ state is less severe than that of the $B^2\Sigma^-$ state; lifetimes of the C state are in the range 3−10 ns. Hence, it appears that diminished line intensity for $J'$ greater than 23 in the C−X progression is due mainly to decreased population and transition moment rather than to predissociation. The advantage of TC-RFWM to detect highly predissociative levels is thus less prominent in the case of C−X than for the B−X transition. Nevertheless, the advantage of interference-free detection associated with the double-resonance nature of TC-RFWM is clearly demonstrated by the detection of resolved lines of the (1−1) band. Many lines of the C−X (1−1) band are overlapped with those of the (0−0) band of CH and the $C^3\Pi-B^3\Sigma$ band of $N_2$ impurity in previous work. With TC-RFWM, one marks a specific lower state via the A−X transition; only when the wavelength of the grating beams coincides with a transition of C−X initiating from the marked state is a signal observed. Interference due to other states or species is thus eliminated.

**1. Spectral Parameters of the $C^2\Sigma^+$ State.** Observed wavenumbers of the C−X (1−1) lines are fitted to an effective Hamiltonian of Brown et al.[29] Matrix elements for $^2\Sigma^+$ and $^2\Pi$ states are given by Amiot et al.[30] with corrections for $\gamma$, $\gamma_D$ of the $^2\Sigma^+$ state reported by Douay et al.[31] There are 13 parameters ($B$, $D$, $H$, $L$, $A$, $\gamma$, $\gamma_D$, $p$, $p_D$, $p_H$, $q$, $q_D$, and $q_H$) that serve to described levels in the ground state. These symbols convey the conventional meaning: $B$, $D$, $H$, and $L$ as rotational and centrifugal distortion parameters, $A$ for spin−orbit interaction,

**TABLE 1: Wave Numbers ($cm^{-1}$) of Lines Observed in the Band $C^2\Sigma^+-X^2\Pi(1\text{-}1)$ of CH**

| $N''$ | $P_1(N'')$ | $o-c^a$ | $P_2(N'')$ | $o-c$ | $Q_1(N'')$ | $o-c$ | $Q_2(N'')$ | $o-c$ | $R_1(N'')$ | $o-c$ | $R_2(N'')$ | $o-c$ |
|---|---|---|---|---|---|---|---|---|---|---|---|---|
| 1 | 31639.27 | 11 | | | | | | | 31720.19 | −4 | | |
| 2 | 31612.84 | −2 | 31618.69 | −1 | 31667.18 | 14 | 31672.83 | −10 | 31747.71 | −11 | 31753.49 | −10 |
| 3 | 31585.65 | 6 | 31589.45 | 2 | 31666.96 | 8 | 31670.76 | −3 | 31774.38 | 16 | 31777.98 | −1 |
| 4 | 31557.79 | −3 | 31560.62 | 0 | 31666.26 | 9 | 31669.02 | −5 | 31799.89 | 5 | 31802.57 | 0 |
| 5 | 31529.57 | −13 | 31531.83 | 0 | 31665.01 | 1 | 31667.22 | −5 | 31824.63 | −11 | 31826.76 | −4 |
| 6 | 31501.21 | −7 | 31502.95 | 2 | 31663.41 | 0 | 31665.26 | 3 | 31848.96 | 8 | 31850.48 | 1 |
| 7 | 31472.59 | 0 | 31473.83 | −5 | 31661.40 | 3 | 31662.85 | −1 | 31872.31 | 8 | 31873.52 | 7 |
| 8 | 31443.66 | 2 | 31444.65 | 2 | 31658.79 | −5 | 31660.08 | 1 | 31894.77 | 7 | 31895.61 | −2 |
| 9 | 31414.43 | 1 | 31415.27 | 10 | 31655.79 | 1 | 31656.74 | −5 | 31916.14 | −7 | 31916.81 | −8 |
| 10 | 31384.91 | 0 | 31385.40 | −5 | 31652.08 | −5 | 31653.03 | 7 | 31936.62 | −3 | 31937.08 | −4 |
| 11 | 31355.06 | −3 | 31355.35 | −8 | 31647.87 | 6 | 31648.57 | 9 | 31955.90 | −3 | 31956.13 | −8 |
| 12 | 31324.87 | −3 | 31325.02 | −6 | 31642.85 | 12 | 31643.35 | 9 | 31973.89 | −1 | 31973.97 | −5 |
| 13 | 31294.22 | −9 | 31294.26 | −8 | 31636.91 | 11 | 31637.31 | 10 | 31990.43 | −1 | 31990.43 | 3 |
| 14 | 31263.13 | −11 | 31263.13 | 0 | 31630.07 | 17 | 31630.25 | 5 | 32005.29 | −8 | 32005.27 | 7 |
| 15 | 31231.38 | −15 | 31231.45 | −1 | 31622.05 | 16 | 31622.20 | 10 | 32018.58 | 5 | 32018.22 | −1 |
| 16 | 31199.22 | −8 | 31198.97 | 3 | 31612.64 | 2 | 31612.79 | 6 | 32029.50 | −18 | 32029.14 | −14 |
| 17 | 31166.18 | −1 | 31165.74 | 2 | 31601.97 | 8 | 31602.07 | 15 | 32038.52 | −8 | 32037.96 | −12 |
| 18 | 31132.11 | −2 | 31131.56 | 0 | 31589.49 | 2 | 31589.54 | 11 | 32045.04 | 7 | 32044.37 | 2 |
| 19 | 31096.85 | −5 | 31096.08 | −15 | 31575.08 | −1 | 31575.08 | 11 | 32048.51 | 5 | 32047.74 | 0 |
| 20 | 31060.26 | 0 | 31059.37 | −13 | 31558.38 | −3 | 31558.29 | 6 | 32048.74 | 11 | 32047.83 | 0 |
| 21 | 31021.86 | −5 | 31021.05 | −1 | | | | | 32045.19 | 18 | 32044.22 | 9 |
| 22 | 30981.38 | −9 | 30980.42 | −12 | | | | | 32036.88 | −11 | 32036.01 | −2 |

[a] Denotes observed minus calculated values in units $10^{-2}$ $cm^{-1}$.

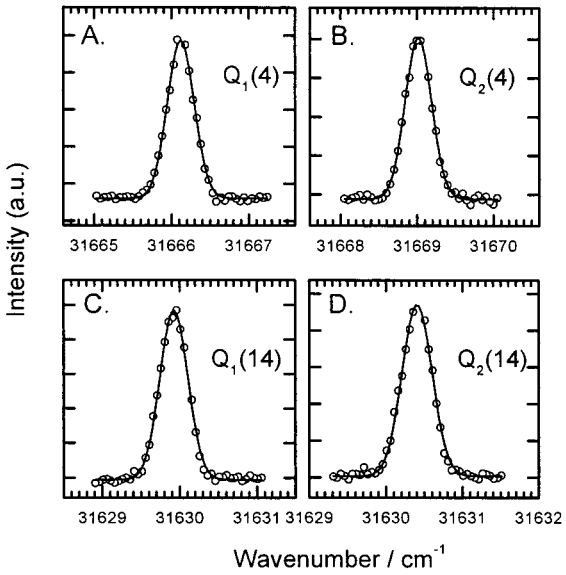


**Figure 2.** Representative TC-RFWM spectra of the C-X system of CH in an oxyacetylene flame with a *YXXY* polarization scheme. Probed A−X lines and wavelengths are: (A) $Q_{1f}$ (4) at 431.326 nm; (B) $Q_{2e}$ (4) at 431.254 nm; (C) $Q_{1f}$ (14) at 430.480 nm; (D) $Q_{2e}$ (4) at 430.493 nm. Laser energies are <10 $\mu$J for each beam.

$\gamma$ and $\gamma_D$ for spin-rotation interactions, and $p$, $p_D$, $p_H$, $q$, $q_D$, and $q_H$ as $\Lambda$-doubling parameters. The term for $L$ in the Hamiltonian is defined as $+LN^4(N+1)^4$. Levels of $C^2\Sigma^+$ $v'=1$ are characterized with seven spectral parameters ($T$, $B$, $D$, $H$, $L$, $\gamma$, $\gamma_D$ ). A fitting program developed in Bernath's group was employed; this program has a provision to exclude a parameter or to constrain it to a particular value for a fit. Only parameters of the $C^2\Sigma^+$ state are allowed to vary during fitting; spectral parameters of the X state are kept invariant to values of Bernath et al.,[9] as their measurements have greater precision and incorporate high-$J$ levels for each vibrational state. During fitting, a precision of line position about 0.2 $cm^{-1}$ is assumed. Residuals between observed and calculated wavenumbers ($o-c$) presented in Table 1 are within experimental accuracy (0.2 $cm^{-1}$) for all lines. We also employed spectral parameters of the $X\ ^2\Pi$ state reported by Zachwieza[10] in the fitting; derived parameters of the C state have similar values, but the variance is slightly greater than that derived with parameters of Bernath et al.[8,9] Derived spectral parameters are tabulated in Table 2. The parameters for $v=1$ of the $C^2\Sigma^+$ state are much improved over those previously reported by Herzberg and Johns.[19]

**TABLE 2: Spectral Parameters ($cm^{-1}$) for States $C^2\Sigma^+$ ($v$ = 0, 1, 2) of CH**

| | this work[a] | ref 19 | ref 17 | ref 32 | ref 20 |
|---|---|---|---|---|---|
| | | | $v=0$ | | |
| $T_0$ | 31791.6467(8) | 31792.4[b] | | 31791.6(1)[b] | 31791.6456(5) |
| $B_0$ | 14.255908(40) | 14.2466(8) | 14.251 | 14.252(1) | 14.25594(34) |
| $D_0/10^{-3}$ | 1.59511(46) | 1.555(5) | 1.551 | 1.565(5) | 1.5962(10) |
| $H_0/10^{-7}$ | 0.767(14) | | | 0.15(4) | 0.824(60) |
| $L_0/10^{-10}$ | −0.373(12) | | | | |
| $\gamma_0/10^{-2}$ | 4.320(32) | 8(2) | | 3.2(2) | 3.9717(11) |
| $\gamma_{D_0}/10^{-5}$ | −3.86(51) | | | −1.7(5) | −2.22(14) |
| $\gamma_{H_0}/10^{-8}$ | 3.09(87) | | | | |
| | | | $v=1$ | | |
| $T_1$ | 34403.106(21) | 34403.7[b] | | | |
| $B_1$ | 13.51614(66) | 13.509(4) | 13.52 | | |
| $D_1/10^{-3}$ | 1.7305(55) | 1.67(5) | 1.70 | | |
| $H_1/10^{-7}$ | 1.47(16) | | | | |
| $L_1/10^{-10}$ | −2.81(15) | | | | |
| $\gamma_1/10^{-2}$ | 3.65(25) | 4(3) | | | |
| $\gamma_{D_1}/10^{-5}$ | −1.32(75) | | | | |
| | | | $v=2$ | | |
| $T_2$ | 36772.825(24) | 36773.1(1)[b] | | 36770.7(1)[b] | |
| $B_2$ | 12.6076(18) | 12.608(5) | | 12.606(6) | |
| $D_2/10^{-3}$ | 2.013(27) | 2.0(0.1) | | 2.00(8) | |
| $\gamma_2/10^{-2}$ | 3.53(43) | 3(1) | | 1.8(8) | |

[a] Uncertainties in parentheses represent one standard deviation in units of the last quoted digit. [b] Reported values are revised to match the Hamiltonian defined by Brown et al.[29] in which the zero energy is set at the virtual $N''=0$ state.

For the C−X (0−0) band, three sets of measurements are available.[17,20,21] Ubachs et al.[20] performed measurements with the best resolution, but they did not include the P and R branches with $N' \geq 12$ in their fitting. The measurements of Bembenek et al.[21] are less accurate; about 40% of the lines reported by them were not included in their fitting because the errors were greater than three standard deviations. Neither set of molecular parameters reported previously incorporated measurements from Heimer[17] with $N'$ up to 28. Whereas uncertainties of measurements from Ubachs et al.[20] and from Bembenek et al.[21] are stated

**TABLE 3: Equilibrium Spectral Parameters[a] of the $C^2\Sigma^+$ State of CH**

| parameters | this work | ref 17 | ref 19 |
|---|---|---|---|
| $B_e$ ($cm^{-1}$) | 14.625 | 14.62 | 14.603 |
| $\alpha_e$ ($cm^{-1}$) | 0.740 | 0.73 | 0.7185 |
| $D_e/10^{-3}$ ($cm^{-1}$) | 1.527 | 1.48 | |
| $\beta_e/10^{-3}$ ($cm^{-1}$) | 0.135 | 0.15 | |
| $r_e$ (Å) | 1.113 | 1.112 | 1.114 |
| $\omega_e$ ($cm^{-1}$) | 2853.2 | 2906 | 2840.2[b] |
| $\omega_e x_e$ ($cm^{-1}$) | 120.9 | 102 | 125.96[b] |

[a] The definitions are $B_v = B_e - \alpha_e(v + 1/2)$ and $D_v = D_e + \beta_e(v + 1/2)$. [b] $E_v = 2840.2(v + 1/2) - 125.96(v + 1/2)^2 + 13.55(v + 1/2)^3 - 3.957(v + 1/2)^4$ based on data of CD and isotopic relations.

(0.00033 and 0.02 $cm^{-1}$, respectively), Heimer's[17] measurements have unknown accuracy. By comparison with values associated with smaller $N'$, we estimate that the accuracy of his measurement is ~0.2 $cm^{-1}$. We fitted the (0−0) transitions with the combined data. Wherever possible, highly accurate spectral lines from Ubachs et al. are used to replace Heimer's in the fitting, but lines from Bembenek et al. are not used. Spectral parameters derived from the combined data of the C−X (0−0) band are listed in Table 2 and compared with previous values. Spectral parameters derived in this work are similar to those reported by Ubachs et al. but are presumably improved slightly because of incorporation of lines associated with high $N'$. The value of $H_0$ reported by Ubachs et al. is modified because of the addition of a parameter $L_0$.

Measurements from Herzberg and Johns[19] for the C−X (2−2) band were also fitted with the present Hamiltonian with improved spectral parameters of the $X^2\Pi$ ($v = 2$) state.[9] Spectral parameters thus derived are slightly improved over previous values,[19,32] as listed in Table 2. We tried to measure the C−X (2−2) band with TC-RFWM, but the signal was weak and only transitions to lower $J'$ were observed. We might be limited by the flame temperature (~2500 K), at which less than 4% of the population is at $v = 2$ of $X^2\Pi$ state. The intensity of the TC-RFWM signal depends on the square of the concentration.[25] Herzberg and Johns[19] employed flash photolysis of diazomethane to produce CH; the C−X (2−2) absorption band was observed at brief delays after photolysis, presumably a large fraction of CH is still in the $v'' = 2$ state. Recent theoretical calculations also indicate that the oscillator strengths to higher vibrational levels of the C state are at least 2 orders of magnitude smaller than that of the C−X (0−0) band, $8.4 \times 10^{-3}$.

We estimate the equilibrium spectral parameters of the $C^2\Sigma^+$ state from Table 2. Because the rotational parameters of the $v'' = 2$ state are less certain, only those of $v = 0$ and $v = 1$ are used to derive $B_e$, $\alpha_e$, $D_e$, and $\beta_e$, as listed in Table 3. The equilibrium distance $r_e = 1.113$ Å for the C state is consistent with previous reports. The anharmonicity of 120.9 $cm^{-1}$ is much greater than those of the A and X states (96.6 and 63.0 $cm^{-1}$, respectively), consistent with the much smaller dissociation barrier for the C state.

**2. Predissociation of the C State.** For all lines of the C−X (1−1) band, the line widths are nearly invariant ($0.36 \pm 0.04$ $cm^{-1}$); some of the line profiles are illustrated in Figure 2. The width is presumably due to the line widths of the lasers and the Doppler width (~0.34 $cm^{-1}$ at 2500 K). With this limitation, only an increase in line width greater than 0.1 $cm^{-1}$ (corresponding to a lifetime of <50 ps) may be accurately determined in our experiments. Ubachs et al.[20] employed a narrow-band laser and determined that the lifetime of the $F_1$ states of $C^2\Sigma^+$ ($v = 0$) is $3.7 \pm 1.0$ ns, independent of $N$ values, whereas that of the $F_2$ states increases slightly with $N$ and reaches $8.0 \pm 1.5$ ns at $N = 11$.

**TABLE 4: Calculated and Experimental Predissociation Line Width Due to Tunneling for Various Rotational Levels of the B and C States ($v = 0$ and 1) of CH**

| | | $B^2\Sigma^-$ | | | | | $C^2\Sigma^+$ | | |
|---|---|---|---|---|---|---|---|---|---|
| | | width ($cm^{-1}$) | | | | | width ($cm^{-1}$) | | |
| $v$ | $N$ | calcd[a] | revised[b] | exptl[c] | $v$ | $N$ | calcd[a] | revised[b] | exptl |
| 0 | 14 | 0.00 | 0.000 | | 0 | 26 | 0.00 | 0.000 | $<2 \times 10^{-3}$ [d] |
| | 15 | 0.01 | 0.000 | | | 27 | 0.01 | 0.000 | |
| | 16 | 0.07 | 0.000 | | | 28 | 0.06 | 0.002 | |
| | 17 | 0.40 | 0.000 | <0.1 | | 29 | 0.21 | 0.001 | |
| | 18 | 1.71 | 0.000 | <0.1 | | 30 | 0.71 | 0.047 | |
| | 19 | 5.41 | 0.002 | $0.54 \pm 0.06$ | | | | | |
| | 20 | 12.9 | 0.020 | $1.9 \pm 0.5$ | | | | | |
| | 21 | 25.5 | 0.127 | $\sim 4.6 \pm 1.0$ | | | | | |
| | 22 | 43.8 | 0.62 | | | | | | |
| | 23 | 68.0 | 2.28 | | | | | | |
| 1 | 0 | 0.39 | 0.000 | | 1 | 17 | 0.00 | 0.000 | |
| | 1 | 0.45 | 0.000 | | | 18 | 0.01 | 0.000 | |
| | 2 | 0.59 | 0.000 | | | 19 | 0.05 | 0.001 | |
| | 3 | 0.88 | 0.000 | | | 20 | 0.17 | 0.006 | |
| | 4 | 1.47 | 0.000 | | | 21 | 0.51 | 0.027 | <0.1[e] |
| | 5 | 2.67 | 0.000 | | | 22 | 1.38 | 0.10 | <0.1 |
| | 6 | 5.18 | 0.000 | | | 23 | 3.40 | 0.31 | <0.1 |
| | 7 | 10.4 | 0.002 | | | 24 | 7.72 | 0.88 | |
| | 8 | 20.7 | 0.007 | <0.1 | | 25 | 16.3 | 2.28 | |
| | 9 | 39.4 | 0.026 | <0.1 | | | | | |
| | 10 | 66.9 | 0.104 | $0.38 \pm 0.05$ | | | | | |
| | 11 | 96.3 | 0.40 | $0.6 \pm 0.2$ | | | | | |
| | 12 | 127.2 | 1.41 | $\sim 3.1 \pm 0.5$ | | | | | |
| | 13 | 158.8 | 4.48 | $\sim 6 \pm 1$ | | | | | |

[a] The potential energy surfaces reported by van Dishoeck (ref 33) are used; the barriers are underestimated. See text. [b] Using revised potential energy surfaces. See text. [c] Experimental values, ref 26. [d] Below $N = 11$, the $F_1$ states have a constant lifetime of $3.7 \pm 1.0$ ns, whereas the $F_2$ states have a lifetime increasing from ~4 to ~8 ns as $N$ increases (ref 20). [e] Experimental value, this work.

The theoretical radiative lifetime (~85 ns) of the $C^2\Sigma^+$ ($v = 0$) state[33] is much greater than the experimental lifetime at low $N$, supporting the suggestion that all levels of the C state are predissociative.[17,19,22,23] Although the potential energy surface of the $C^2\Sigma^+$ state intersects with the $1^4\Pi$ state, the crossing point is nearly at the barrier height that results from avoided crossing of the $C^2\Sigma^+$ and $2^2\Sigma^+$ states.[33] Hence, the contribution of the spin−orbit coupling between the $C^2\Sigma^+$ and $1^4\Pi$ states to predissociation to $v = 0$ and 1 levels is very small. Oscillator strengths for absorption into higher vibrational states are also small. Herzberg and Johns[19] suggested that the coupling between the $C^2\Sigma^+$ and $B^2\Sigma^-$ states causes the predissociation. Theoretical calculations[33] indicated that such a coupling might be the cause of predissociation provided that the spin−orbit coupling matrix element is of the order of 10 $cm^{-1}$.

We have observed predissociation of the $B^2\Sigma^-$ state using a similar experimental technique;[25,26] the width increases drastically for lines associated with levels $N' > 19$ and $N' > 10$ for $v' = 0$ and 1, respectively. The predissociation has been interpreted with tunneling through the barrier dissociation. Using the ab initio potential energy surfaces of the B and C states reported by van Dishoeck,[33] we calculated the predissociation line width listed in Table 4 for various rotational levels with a program "LEVEL" developed by LeRoy.[34] Because the well depths of both B and C states are underestimated by ab initio calculations (0.29 vs 0.43 eV and 0.86 vs 0.96 eV for ab initio vs experimental values of the B and C states, respectively), predicted threshold $N'$ values for tunneling are smaller than experimental values. When we increase the well depth to the

experimental value, predicted predissociation line widths fit satisfactorily with experimental observation. It is clear that the threshold $N'$ values for tunneling are greater than $N' = 28$ and 20, respectively, for the $C^2\Sigma^+$ ($v' = 0$ and 1) states. For all observed lines (associated with $N' \leq 23$ of $C^2\Sigma^+$ ($v = 1$)), we observed negligible broadening, consistent with the prediction. Hence, it is clear that tunneling has little contribution to predissociation of all rotational levels observed in this work.

## Conclusions

We measured 124 lines of the C−X (1−1) band of CH in an oxyacetylene flame with the TC-RFWM technique; six branches of this system are resolved for the first time. We fitted the wavenumbers of these lines to provide accurate spectral parameters for the $C^2\Sigma^+$ ($v = 1$) state. Improved parameters are also obtained for the $v = 0$ and 2 states; hence, equilibrium values are estimated. For all observed rovibronic transitions, the line widths showed negligible broadening. The cause of this weak predissociation is coupling of the $C^2\Sigma^+$ and $B^2\Sigma^-$ states, rather than curve-crossing by the $1^4\Pi$ state or rotational tunneling.

**Acknowledgment.** The authors thank Professors P. F. Bernath, for providing his spectral fitting program, and R. J. LeRoy, for providing his LEVEL program. A. Kumar thanks the National Tsing Hua University for a postdoctoral fellowship. This work is supported by the National Science Council of the Republic of China (Grant NSC88-2113-M-007-001).

## References and Notes

(1) Mélen, F.; Grevesse, N.; Sauval, A. J.; Farmer, C. B.; Norton, R. H.; Bredohl, H.; Dubois, I. *J. Mol. Spectrosc.* **1989**, *134*, 305 and references therein.
(2) Rydbeck, O.; Ellder, J.; Irvine, W.; Sume, A.; Hjalmarson, A. *Astron. Astrophys.* **1974**, *33*, 315 and references therein.
(3) Nicolet, M. *Z. Astrophys.* **1938**, *15*, 145.
(4) Rensberger, K. J.; Dyer, M. J.; Copeland, R. A. *Appl. Opt.* **1988**, *27*, 3679 and references therein.
(5) Bass, A. M.; Broida, H. P. In *Natl. Bur. Stand. Monograph 24*; U.S. Natl. Bur. Stand.: Washington, DC, 1961; pp 1−20.
(6) Bembenek, Z.; Kepa, R.; Para, A.; Rytel, M.; Zachwieja, M.; Janjic, J. D.; Marx, E. *J. Mol. Spectrosc.* **1990**, *139*, 1.
(7) Para, A. *J. Phys. B* **1991**, *24*, 3179.
(8) Bernath, P. F. *J. Chem. Phys.* **1987**, *86*, 4838.
(9) Bernath, P. F.; Brazier, C. R.; Olsen, T.; Hailey, R.; Fernando, W. T. M. L.; Woods, Ch.; Hardwick, J. L. *J. Mol. Spectrosc.* **1991**, *147*, 16; **1991**, *149*, 563; **1994**, *165*, 301.
(10) Zachwieja, M. *J. Mol. Spectrosc.* **1995**, *170*, 285.
(11) Fortrat, M. R. *C. R. Acad. Sci. (Paris)* **1924**, *178*, 1272.
(12) Hori, T. *Z. Phys.* **1929**, *59*, 91.
(13) Moore, C. E.; Broida, H. P. *J. Res. Natl. Bur. Stand. (U.S.) A* **1959**, *63*, 19.
(14) Elander, N.; Smith, W. N. H. *Astrophys. J.* **1973**, *184*, 663.
(15) Hirano, A.; Ipponmatsu, M.; Tsujishita, M. *Opt. Lett.* **1992**, *17*, 303.
(16) Tsujishita, M.; Ipponmatsu, M.; Hirano, A. *Jpn. J. Appl. Phys.* **1993**, *32*, 5564.
(17) Heimer, T. *Z. Phys.* **1932,** *78*, 771.
(18) Gerö, L. *Z. Phys.* **1941**, *117*, 709.
(19) Herzberg, G.; Johns, J. W. C. *Astrophys. J.* **1969**, *158*, 399.
(20) Ubachs, W.; Meyer, G.; ter Meulen, J. J.; Dymanus, A. *J. Chem. Phys.* **1986**, *84*, 3032.
(21) Bembenek, Z.; Kepa, R.; Rytel. M. *J. Mol. Spectrosc.* **1997**, *183*, 1.
(22) Hesser, J.; Lutz, B. *Astrophys. J.* **1970**, *158*, 703.
(23) Brzozowski, J.; Bunker, P.; Elander, N.; Erman, P. *Astrophys. J.* **1976**, *207*, 414.
(24) Ortiz, M.; Campos, J. *Physica C* **1982**, *114*, 135.
(25) Hung. W.-C.; Huang, M.-L.; Lee, Y.-C.; Lee, Y.-P. *J. Chem. Phys.* **1995**, *103*, 9941.
(26) Kumar, A.; Hsiao, C.-C.; Hung, W.-C.; Lee, Y.-P. *J. Chem. Phys.* **1998**, *109*, 3824.
(27) Eichler, H. J.; Günter, P.; Rohl, D. W. *Laser-Induced Dynamic Gratings*; Springer: Berlin, 1986.
(28) Brown, J. M.; Hougen, J. T.; Huber, K.-P.; Johns, J. W. C.; Kopp, I.; Lefebvre-Brion, H.; Zare, R. N. *J. Mol. Spectrosc.* **1975**, *55*, 500.
(29) Brown, J. M.; Colbourn, E. A.; Watson, J. K. G.; Wayne, F. D. *J. Mol. Spectrosc.* **1979**, *74*, 294.
(30) Amiot, C.; Maillard, J. P.; Chauville, J. *J. Mol. Spectrosc.* **1981**, *87*, 196.
(31) Douay, M.; Rogers, S. A.; Bernath, P. F. *Mol. Phys.* **1998**, *64*, 425.
(32) Botterud, I.; Lofthus, A.; Veseth, L. *Phys. Scr.* **1973**, *8*, 218.
(33) van Dishoeck, E. F. *J. Chem. Phys.* **1987**, *86*, 196.
(34) LeRoy, R. J. *Chemical Physics Research Report CP-555R*; University of Waterloo: Waterloo, Canada, 1996.